Engineering Structures 181 (2019) 427–436

Contents lists available at ScienceDirect

Engineering Structures

journal homepage: www.elsevier.com/locate/engstruct

Seismic response modification factor for steel slit panel-frames

Fatemeh Aliakbari, Hashem Shariatmadar*

Department of Civil Engineering, Ferdowsi University of Mashhad, Mashhad, Iran

ARTICLE INFO

Keywords:
Seismic response modification factor
Overstrength factor
Ductility factor
Steel slit panel-frames
Dual moment-resistant frames

ABSTRACT

In this paper, the overstrength, ductility and response modification factors of moment resistant frame (MRF) with steel vertical slit panel (SSP-MRF) were investigated and determined. For this purpose, buildings with various stories were used. Abaqus software was used to perform the static pushover analysis, linear dynamic analysis, and nonlinear incremental dynamic analysis. In this research, seismic response modification factor has been evaluated for each model structure using pushover analysis, and the tentative value 8.11 has been proposed for the ultimate limit state design method. Some of the results of pushover analysis and nonlinear incremental dynamic analyses were compared. According to this comparison, the response modification factor of 10-story model structure derived from pushover analysis (6.14) was slightly smaller than those obtained from incremental dynamic analyses (7.5).

1. Introduction

Devastating earthquakes show how vulnerable humans are against natural powers. Hence, one of the main challenges in earthquake and structural engineering is to develop innovative engineering ideas to protect the structures and their inhabitants.

Intermediate to specific moment-resistant frame systems are ductile. However, they do not provide sufficient lateral stiffness [1]. Increasing the cross-sectional area to control lateral displacement is not economic. As a result, using shear walls or bracings beside moment frames decreases moment frame sections and increases the stiffness. However, the excessive stiffness of the concrete shear wall and unsuitable bending behavior in short structures result in a decrease in ductility. For the first time, slit concrete shear walls with energy dissipation capability were proposed in 1968 [2]. In 1999, the ductility of the slit walls was examined using reinforced concrete shear connectors [3]. Slit concrete shear walls have a better ductility but a lower strength compared to ordinary concrete shear walls. Furthermore, reinforced concrete is damaged quickly against cyclic plastic deformations. These factors prevented from grooving concrete shear walls [4].

Many different lateral load-carrying systems are used in seismic zones and the steel slit panel (referred to SSP, henceforth) and the steel slit panel-frame (SSPF) are known as one of these systems. The steel plate shear walls with slits have been utilized in steel and composite structures in Japan, including building with 7–19 stories [5]. Scholars have offered some of the most important benefits of this system as follows [6,7]: (a) stable and ductile behavior; (b) the stiffness and strength of the SSP can be controlled by varying the slit design independently of each other; (c) the full beam span does not have to be occupied by the SSP; (d) simple fabrication and installation; (e) feasibility of seismic retrofitting.

Seismic codes reduce the design load using the fact that the structures have substantial reserve strength and the energy dissipation capacity. Structural designs include the overstrength and the ductility through a response modification factor. The response modification factor is the ratio of shear force that must be resisted by the structure if it remains completely elastic to shear force corresponding to the formation of first plastic hinge [8,9]. Therefore, obtaining these seismic coefficients to replace linear analysis methods rather than nonlinear analysis is highly important in structural and earthquake engineering.

The present research is aimed at evaluating overstrength, force decrease due to ductility, and response modification factors of the moment resisting frames with steel slit panels (SSP-MRF) designed according to Iranian Earthquake Resistant Design Code [10] and Iranian National Building Code (part 10) for Structural Steel Design [11].

2. Steel plate shear walls with vertical slits

2.1. General

Steel shear walls with vertical slits were studied as a new type of seismic load-carrying elements in 2003 [6]. In this system, steel strips between slits act as a series of bending links that resist large bending deformations compared to shear deformations and provide a ductility

* Corresponding author at: Department of Civil Engineering, Ferdowsi University of Mashhad, Azadi Square, Mashhad, Iran.
E-mail addresses: fatemeh.aliakbari@mail.um.ac.ir (F. Aliakbari), shariatmadar@um.ac.ir (H. Shariatmadar).

https://doi.org/10.1016/j.engstruct.2018.12.027
Received 16 May 2018; Received in revised form 10 November 2018; Accepted 10 December 2018
0141-0296/ © 2018 Elsevier Ltd. All rights reserved.

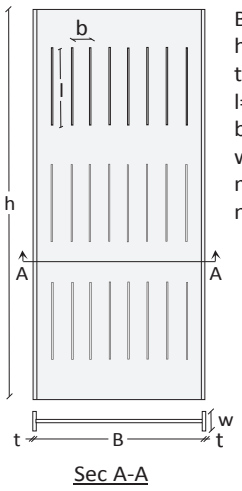

B= width of wall
h= heigh of wall
t= thickness of wall
l= heigh of link
b= width of link
w= edge stiffner width
m= number of row
n= number of links per row

Fig. 1. Geometrical characteristics of a steel slit panel with a vertical slit.

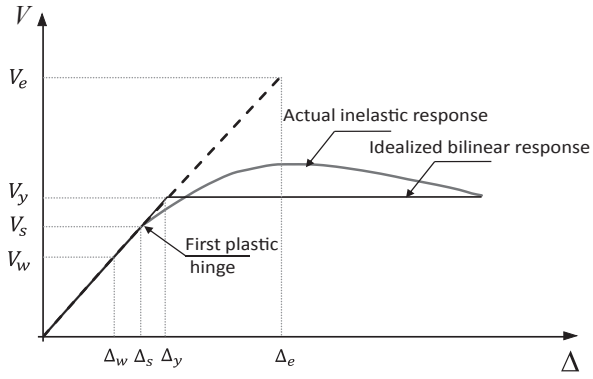

Fig. 2. General structure response [15].

Table 1
Specimen properties.

Beam property	t (mm)	b (mm)	l (mm)	h (mm)	B (mm)
W6×9	4.8	50.8	254	1168	500

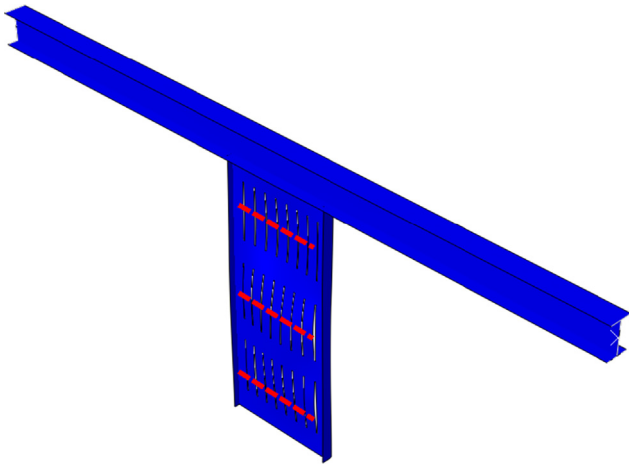

Fig. 4. Final initial geometrical model of SSPF.

Table 2
Imperfections in test and analytical model (SSPF) (Unit: mm).

	Upper row	Middle row	Lower row
Test	1.60	11.10	3.20
Model	1.48	11.42	2.92

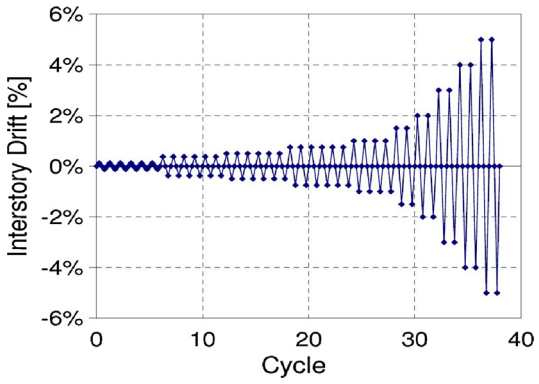

Fig. 5. The loading pattern, Cortes and Liu [12].

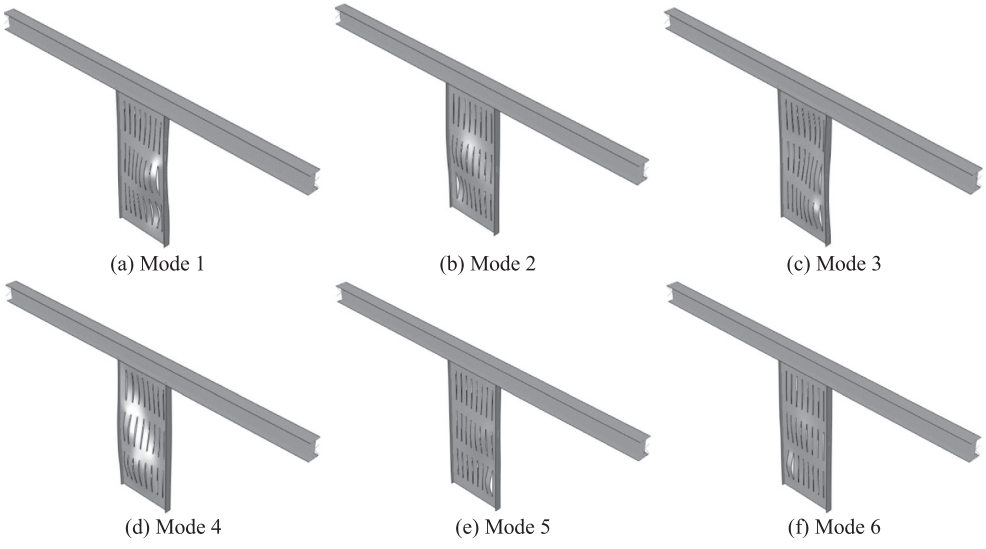

Fig. 3. Buckling mode shapes of SSPF.

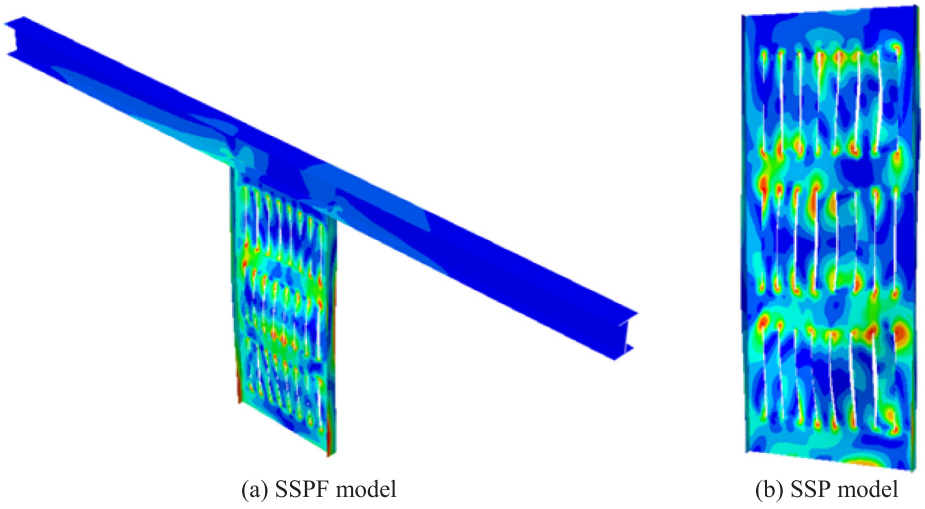

Fig. 6. Finite element models.

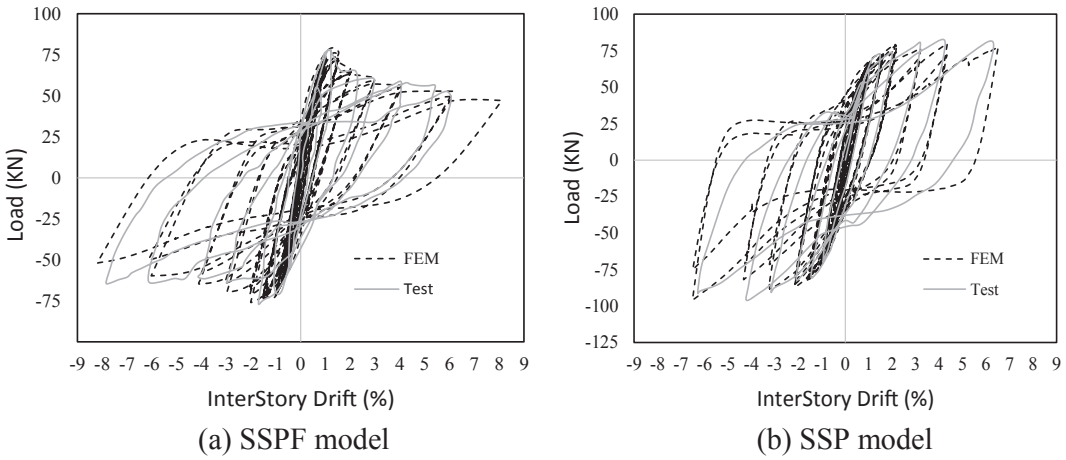

Fig. 7. Hysteresis curves of the experimental and numerical models.

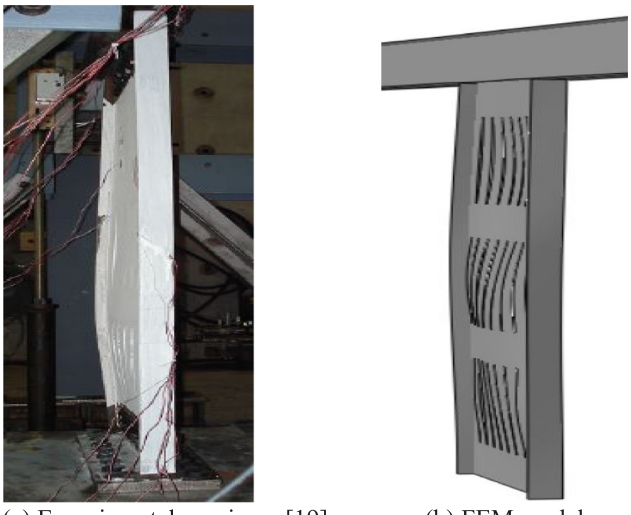

Fig. 8. Out of plane buckling at 1.5% Interstory Drift in the SSPF model.

response without needing to provide significant stiffness. In fact, links behave like beams in double curvature and dissipate a significant amount of energy by forming plastic hinges at their ends. Fig. 1 shows an SSP together with its edge stiffeners. Edge stiffeners increase the strength and stiffness of panel and play an important role in supplying out-of-panel stability [12].

2.2. Design parameters of SSPs

There are three basic parameters that lead to the ductile behavior of an SSP [6]. The parameters include α, β and b/t that are related to the geometrical properties of SSP. The geometry of an SSP and all of its parameters are displayed in Fig. 1 where α denotes the shear span aspect ratio that is defined as the length to width (l/b) ratio of the link and β is determined as ml/h (previous researches have examined the recommended range of the parameters). It should be highlighted that α ranges from 2.5 to 5.0, the link's cross-section aspect ratio (b/t) ranges from 10 to 15, and it is recommended that β to be between 0.65 and 0.85 [13]. Researches show that selecting a suitable range for the parameters leads to a ductile behavior and high energy dissipation in the system.

In an SSP, the sum of the bending strengths of the links and edge stiffeners forms the bending strength of SSP (Q_{ult}). Moreover, lateral-torsional buckling (LTB) that may occur in the link or in the panel is not desirable, because the panel's strength must be chosen at a level that plastic hinges develop at the end of the links. Thus, the minimum of the Q_{ult} and Q_{LTB} indicates the capacity of the panel (Q_{panel}). Their relations are defined as follows [12]:

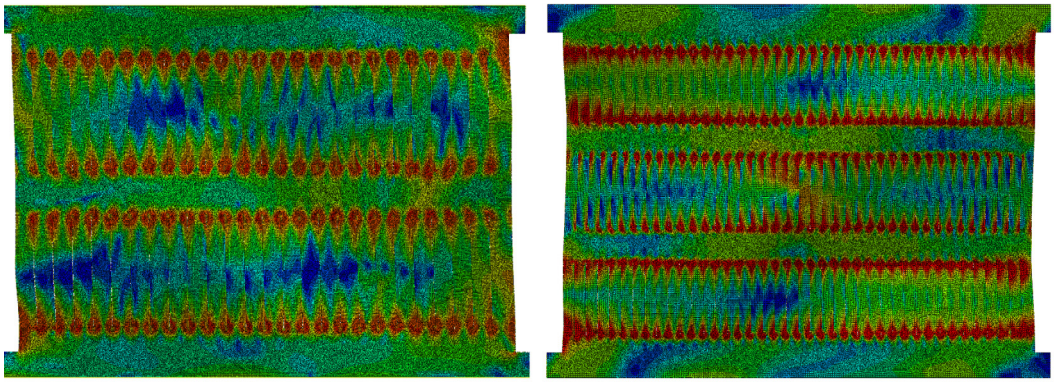

(a) Specimen 1 (b) Specimen 2

Fig. 9. Finite element models.

Table 3
Summary of Specimens.

Specimen	Material	l (mm)	b (mm)	t (mm)	m	α	β
1	LYP100	410	70.3	9	2	5.8	0.71
2	LYP100	267	45.5	9	3	5.9	0.70

$$Q_{ult} = \frac{F_y t}{2l}[b^2 n + 2b^2(t-1) + 2w_{es}(2b+t)] \quad (\text{if } W_{es} > b) \tag{1}$$

$$Q_{ult} = \frac{F_y t}{2l}[b^2 n + 4bw_{es} + 2w_{es}{}^2] \quad (\text{if } w_{es} < b) \tag{2}$$

$$Q_{LTB} = \left[\frac{4.013}{\left(\frac{h_{LTB}}{2}\right)^2}\right]\sqrt{EI_{panel}C} \tag{3}$$

where the yield strength of the steel is presented by F_y, the moment of inertia of the panel (assuming no slit and considering edge stiffeners) about its weak axis is presented by I_{panel}, the torsional constant is presented by C (as in Eq. (4)), the height of the panel to the geometric center of the bolt group is presented by h_{LTB} and Young's modulus is presented by E. It is assumed in Eqs. (1) and (2) that the thickness of the edge stiffeners and the main plate are similar [12].

$$C = GJ = \left(\frac{Gt^3}{3}\right)(2w + B - 2t) \tag{4}$$

where the shear modulus is denoted by G and other parameters in Eqs. (1)–(4) are given in Fig. 1. Additionally, the stiffness of an SSP can be defined according to the bandzone stiffness, shear stiffness of the links and bending stiffness of the links using Eq. (5), as follows [12]:

$$K = \frac{1}{\frac{k(h-ml)}{GBt} + \frac{m}{n}\left(\frac{kl}{Gbt}\right) + k(\alpha)\left(\frac{m}{n}\right)\left(\frac{l^3}{Etb^3}\right)} \tag{5}$$

where k is the shear deformation shape factor. For a rectangular section, k is 1.2, and k(α) is given by Eq. (6):

$$K(\alpha) = (1 + \alpha^{-1})^3 \tag{6}$$

3. Response modification factor

After discovering the inelastic and ductile behavior of the structures against earthquake, researchers always wanted to find a simple and accurate method to incorporate the energy dissipation effect of the structure associated with inelastic deformations into their calculations. Three factors including strength, stiffness, and ductility are inelastic seismic requirements of the structure and inelastic analysis is required to consider the three factors in the calculations. Since inelastic analysis is complex and time-consuming, the equivalent elastic analysis is allowed in the codes, and the response modification factor is used.

ATC-19 [14] uses a simple method as the product of three main parameters to determine the response modification factor as shown in Eq. (7):

$$R = R_0 R_\mu R_r \tag{7}$$

R_r is the redundancy factor to consider the reliability of lateral load carrying systems due to the number of resistant frames at any direction of the building. The coefficient is equal to 1.0 in the present study. R_μ is the reduction factor due to the ductility that shows the ductility capacity of the structure in the nonlinear range of the materials. In fact, if a structure does not have the ductility capacity, no response modification

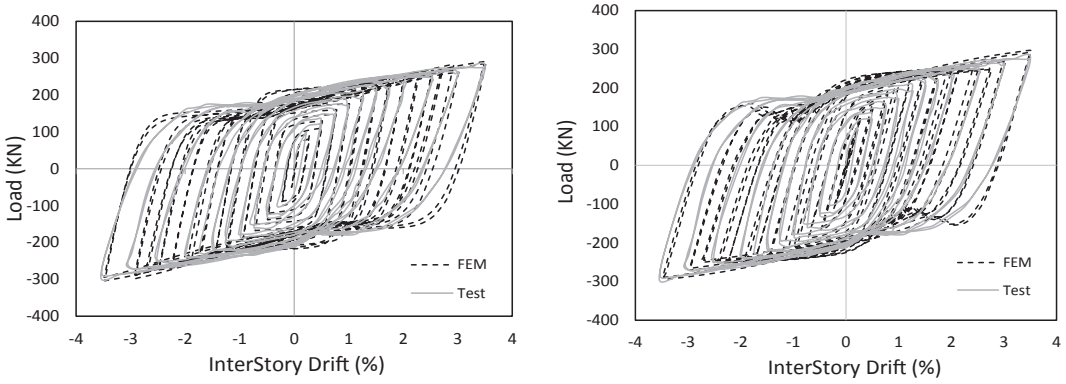

(a) Specimen 1 (b) Specimen 2

Fig. 10. Hysteresis curves of the experimental and numerical models.

Table 4
Full scaled panel properties.

m	n	B (mm)	h (mm)	l (mm)	b (mm)	t (mm)	w_{es}(mm)
3	9	1500	3500	760	160	11	150

Table 5
Principal parameters in full scaled panel geometry.

parameters	Actual value	Ideal range
α	4.75	2.5–5
β	0.65	0.65–0.85
b/t	14.54	10–15

factor can be defined for it. The value of R_μ is directly related to the ductility capacity of the structural members such as beams, columns, bracings, and shear walls. R_0 is the overstrength factor. The overstrength factor is an important factor to increase the response modification factor in systems with multiple freedom degrees.

Fig. 2 represents the base-shear versus roof displacement relation of a structure.

The ductility factor R_μ and the overstrength factor R_0 are defined by Eq. (8).

$$R_\mu = \frac{V_e}{Vy}$$
$$R_0 = \frac{V_y}{V_S} \tag{8}$$

where V_S is the base shear corresponding to the first separation point of the roof displacement-base shear curve of the nonlinear structure from the same structure, but with a linear behavior, Vy is the yield force of the structure, Δ_y is yield displacement and V_e is the shear force that must be resisted by the structure once it does not show any inelastic behavior and remains elastic. If it is possible to design the structure based on the allowable stress method, the design codes reduce the design force from V_s to V_w. In other words, the response modification factor is multiplied by Y (see Eq. (9)) [15].

$$Y = \frac{V_s}{V_w} \tag{9}$$

In the present study, the ultimate strength design method is used. Hence, the behavior factor is calculated as follows:

$$R = \frac{V_e}{V_s} = \frac{Ve}{Vy} \times \frac{V_y}{V_s} = R_\mu \times R_s \tag{10}$$

4. Numerical model and verification

In this section, a valid finite element model is presented to model the behavior of an SSP and an SSPF, and the results of the numerical model are compared with the experimental results of other researches. The finite element (FE) software Abaqus is used to perform the analyses. In the present article, the specimens tested in the study by Cortes and Liu [12] (PA-1 and PF-1) and He et al. [16] (Specimens 1 and 2) are used to verify the proposed behavior model. In the study conducted by Cortes and Liu on steel slit shear walls, they examined two groups of test specimens including Steel Slit Panels (SSPs) and Steel Slit Panel-Frame (SSPF). The models were prepared and tested at the 1/3 scale. The overall height of the wall was 1168 mm, its width was 500 mm, and its thickness was 4.8 mm. Furthermore, the wall plate had three rows of slits, with 8 strips at any row. The geometrical properties of the SSPF are given in Table 1. According to the experiments performed by Cortes and Liu, the panel used in the SSPF was the panel modeled independently (PA-1).

The SSP and SSPF were modeled using shell element (S4R). The combined stiffening model was used to define the stiffening model of material. The out-of-plane buckling is one of the main factors of the strength reduction of the steel slit wall [6]. The initial stiffness and strength are decreased significantly by initial imperfections [17,18]. Imperfections are created in structural members in different ways (imperfections can be caused by the residual stresses induced when the edge stiffeners are welded [19]). In the experimental specimens, the SSP model (PA-1 specimen in the study by Cortes and Liu [12,19]) had an initial imperfection; the links in the upper and lower row had a maximum of 4.8 mm out-of-plane deformation at link mid-height, measured relative to a line connecting the 1st and 9th link in a row. The links in the middle row had the same amount of deformation but towards the opposite side. Furthermore, in the SSPF model (PF-1 specimen in the study by Cortes and Liu [12,19]) the panel's initial imperfections, measured relative to a horizontal line connecting the 1st and 9th link in a row, were approximately 1.6 mm in the upper row, 3.2 mm in the lower row, and 11.1 mm in the middle row. The imperfections in the upper and lower row were towards the same side; the imperfection in the middle row was towards the opposite side [12,19]. Hence, at first, buckling analysis was done in the finite element (FE) software Abaqus and the input file was changed to take this phenomenon into account. The obtained buckling shapes for SSPF model are presented in Fig. 3.

After performing buckling analysis using Eigenvalue Method, a combination of all deformations of buckling modes (Fig. 3) with small factors was used as the initial imperfection. The final geometry of an

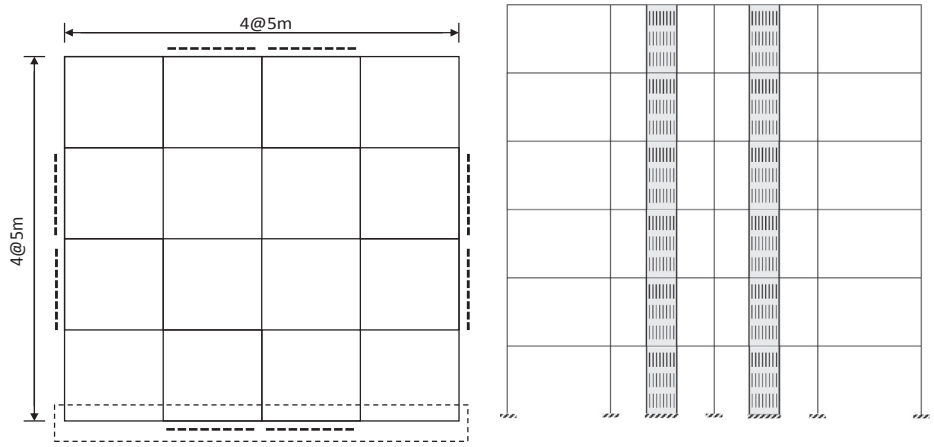

a) Plan b) SSP-MRF

Fig. 11. The configuration of typical model structures.

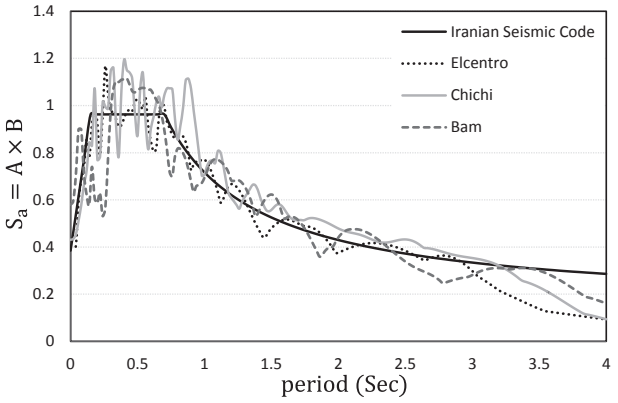

Fig. 12. Variation of spectral with period of structure.

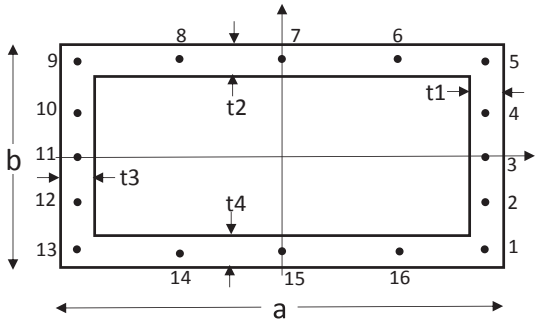

Fig. 13. Location of integration points in a standard box profile [23].

initial SSPF model is presented in Fig. 4.

As a result, initial imperfections are added to the analytical model, in order to increase the similarity between the modeling and reality [20] (see Table 2). If the initial imperfection is not defined in the symmetric member, the member may buckle at larger loads. The buckling is due to slight numerical instabilities that are accumulative, and it must not be mistaken by actual buckling. The results are confirmed when comparing with the experimental findings.

One of the factors that results in strength decline in the slit wall is the stress concentration at the beginning and at the end of slits which leads to the propagation of cracks. Two main mechanisms that result in failures in soft metals include soft failure due to growth and bond of holes, and shear failure due to the accumulation of the shear border [17,21]. Both ductile and shear damages must be modeled correctly in order to be able to model the damage in the finite element software properly. In the present article, the loading pattern of the study by Cortes and Liu [12] which is adopted from ATC-24 [22] is used to compare the experimental results and the numerical analysis results. The loading pattern is shown in Fig. 5. Fig. 6 shows the finite element models used for verification.

The load-displacement relation is compared between the experimental and FEM results in Fig. 7. The hysteresis curves indicate that the finite element models are matched excellently with the experimental results.

The numerical model shows the damage, strength decline, pinching phenomenon, out-of-plane buckling and deformation very well (see Figs. 7 and 8).

In the study by He et al. [16] on steel slit shear walls, they examined four specimens. Specimens 1 to 3 were made with low-yield-point steel (LYP) having a yield stress of 100 MPa and Specimen 4 was made from SS400. In the present article, Specimens 1 and 2 are used to verify the behavior model. Fig. 9 shows the finite element models used for verification. The main parameters of Specimens 1 and 2 are given in Table 3.

The hysteresis curves of the experimental and FEM results are compared in Fig. 10. These indicate that the results of the numerical models are in good agreement with experimental results. Therefore, the modeling is verified by experimental works.

5. Design of model structures

When an SSPF system is chosen as the lateral force resisting system, the panel is selected in the first step.

5.1. SSP design parameters

In the first step of the design of an SSP, the panel thickness, t, its height, h, and its width, B, are defined. The number of links, n, the number of rows, m, and the height of the link, l, are defined in the next step. The range of these parameters for the ductile behavior of an SSP is described in previous sections. Accordingly, an SSP is used with the geometrical dimensions 3 times larger than the initial dimensions whose modeling is verified in the previous section (SSP model). The properties of the SSP and the allowed range of α, β and b/t are presented in Tables 4 and 5, respectively.

5.2. Structural model

To calculate the ductility reduction factor, overstrength factor and the response modification factor of the moment resisting frame with slit steel panel (SSP-MRF), the structures with 3, 6, 10, 12 and 15 stories were designed with the span length of 5 m according to the Iranian Earthquake Code [10] and Iranian National Standard [11]. The height of the stories was selected as 3.5 m. Fig. 11a and b indicates the typical structural models. The dashed lines show the spans with SSP.

For beams and columns design, the equivalent lateral static force (according to the provision of Earthquake Code [10]) was applied on the story levels and ultimate stress design method (according to the part 10 of the Iranian National Code [11]) was used. In addition, the stories'

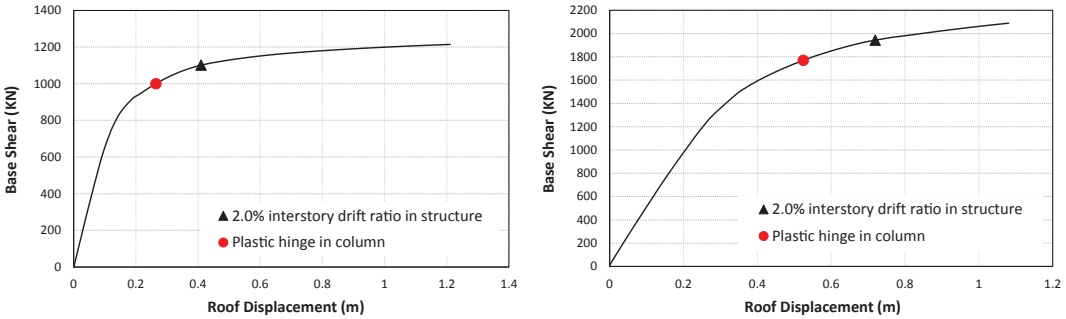

(a) 6-story structure (b) 15-story structure

Fig. 14. Pushover curves for SSP-MRFs.

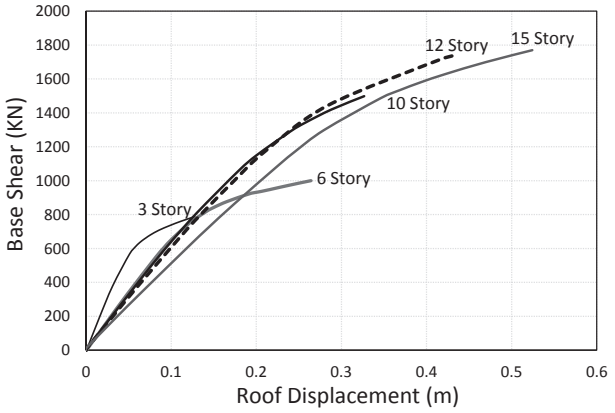

Fig. 15. Roof displacement-base shear curves of SSP-MRFs.

dead and live loads were 590 and 200 kg/m^2, respectively. Besides, the roof's dead and live loads were 570 and 150 kg/m^2, respectively. Eq. (11) was employed to calculate the design base shear as follows:

$$V = CW$$
$$C = \frac{ABI}{R} \tag{11}$$

where the base shear of the structure is denoted by V, the seismic coefficient is denoted by C and the equivalent weight of the structure is denoted by W. The design spectral acceleration is denoted by multiplication A and B (for the soil type and the fundamental period of the structure T (Fig. 12)). To design the frame, the importance factor, I = 1.0, the initial response modification factor, R = 6.5, and the design basis accelerations ratio, A = 0.35 were utilized. The load-carrying system used in the article was a dual system and provisions are stated for its design in the Iranian Standard Code No. 2800. The dual systems are defined in the Iranian Earthquake (Standard Code No. 2800) [10], as follows.

A kind of a structural system in which vertical loads are resisted by building frames and resistance against lateral loads is provided by some shear walls or braced frames together with some moment frames. Moment-resistant and shear walls or braced frames must be able to resist at least 25% and 50% of the lateral forces at the base level, respectively. Furthermore, in buildings with a height less than 30 m, shear walls can be designed for 100% of the lateral load and the moment frame can be designed for 30% of the lateral load instead of the load distribution according to the stiffness of the load-carrying elements. As a result, the main purpose of the present article is to study building frames that can resist the gravity loads and the main lateral load sustain by SSPs, because the experimental results show the high capacity and very ductile behavior of such steel panels. Therefore, the moment frames are designed for the minimum limits that specified by Iranian Standard No. 2800. Also in all buildings, the base shear at each floor (V_i from equivalent static analysis) is divided by the capacity provided by each panel to make sure that the number of panels used at each floor is enough to resist the base shear limit defined by the Iranian Standard No. 2800.

6. Modeling of structure

All analyses were performed by modeling of the structures in Abaqus program. Abaqus software is one of the most powerful finite element simulation software. A wide range of elements can be used in this software. Therefore, it makes the user able to model and analyze different linear and nonlinear problems. Hence, the software is used in the article to model and define the materials, elements, constraints and the structural nonlinear behavior.

Beam elements (B31) are used to model the frame members including beams and columns, whose nodes have three translational degrees of freedom and three rotational degrees of freedom in space. The beam section behavior is calculated in terms of the response of the section to stretching, bending, shear, and torsion. Every cross-section of the beam elements has some integration points that are used to compute the outputs. For example, 16 points are utilized to determine the output of the box profiles (Fig. 13).

The shell element (S4R) is used to model SSP. The S4R element has 6 degrees of freedom in all nodes, including three translational and three rotational DOFs [23]. The steel used to define the material property in the frame is ST37 with nonlinear behavior that is the normal steel used in Iran with the yield stress of 2400 kg/cm^2 and the ultimate stress of 3700 kg/cm^2. To define the characteristics of the material used in SSP, data obtained from the coupon tests were used. Also, the imperfection in the initial model is taken into account to make the results closer to the reality, and a buckling analysis is performed using the eigenvalue method before principal analyses. In addition, the geometrical nonlinearity is incorporated in the analysis that is well controlled by Abaqus software.

7. Nonlinear static analysis of model structures

Many studies have been published which provided information regarding pushover analysis. Once a suitable lateral load distribution is adopted, elastic and the inelastic responses of buildings can be determined by pushover analysis when subjected to earthquake ground motions [24].

7.1. Pushover analysis

At first, eigenvalue buckling analyses were performed and then

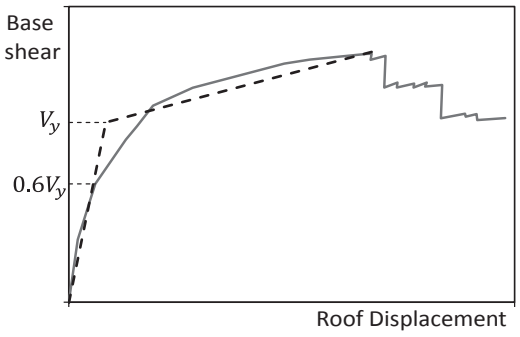

(a) The idealized curve for positive post-yield stiffness

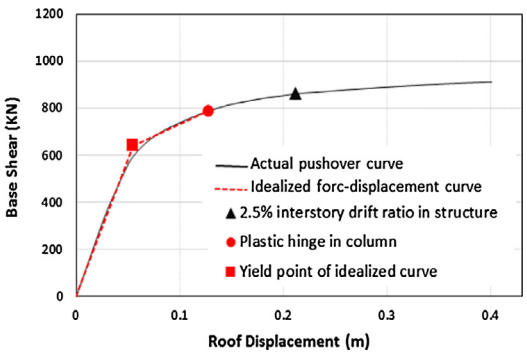

(b) Bilinear represent of three-story SSP-MRF

Fig. 16. Idealized force-displacement curve.

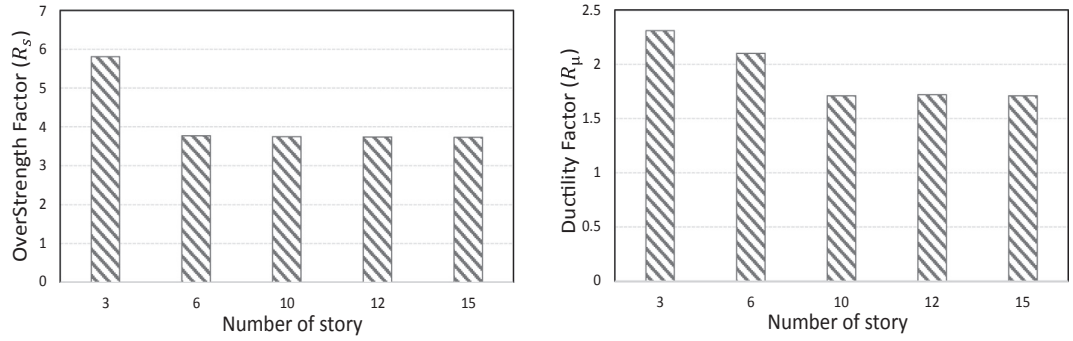

(a) Overstrength factor (b) Ductility factor

Fig. 17. Overstrength and ductility factor of structures.

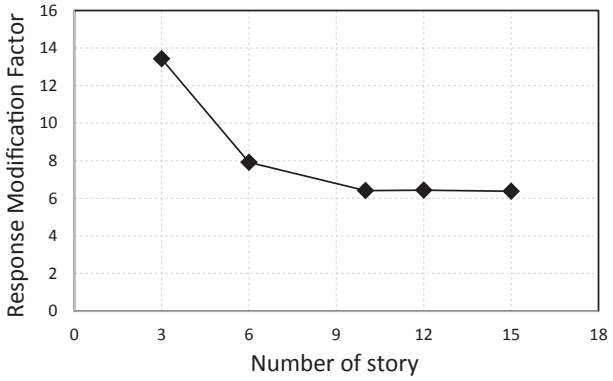

Fig. 18. Response modification factor.

Table 6
Overstrength, ductility and response modification factors of SSP-MRFs from pushover analysis.

No. story	Limit state	R_0	R_μ	R
3	PHC[a]	5.81	2.31	13.42
6	PHC	3.77	2.1	7.91
10	PHC	3.75	1.71	6.41
12	PHC	3.74	1.72	6.43
15	PHC	3.73	1.71	6.38

[a] Plastic hinge in column.

Table 7
Ground motion data.

Earthquake	Year	PGA (g)	Station
Bam	2003	0.166	Abaragh
Chichi	1999	1.009	TCU084
Elcentro	1940	0.319	El Centro Array #9

pushover analyses were carried out by Abaqus software to compute the overstrength and ductility factors for each of the structures by increasing the lateral loads gradually according to the fundamental mode shape (the natural periods and mode shapes of the models are determined by the frequency analyses). The static pushover curves of the 6-story and 15-story structures are shown in Fig. 14.

In the present research, as the following failure criteria were met by the analytical results, the analysis was terminated. The roof displacement-base shear curves of SSP-MRFs that are used in calculating the overstrength and ductility factors are shown in Fig. 15. The comparison of results shows that the overall behaviors for all structures are the same, except for 6-story structure which has a more ductile behavior.

7.2. Failure criteria

The failure criteria were classified into two groups:

7.2.1. The relative displacement between the floors or the inter-story drift

The limit of maximum relative story displacement was controlled according to the Iranian Standard Code No. 2800 as follows [10]:

- In 1–5 story buildings:

$$\Delta_M < 0.025H \tag{12}$$

- In other buildings:

$$\Delta_M < 0.02H. \tag{13}$$

In these relations, H is the story height.

7.2.2. Instability and failure mechanism

To estimate the ultimate limit determined by the maximum inter-story drift ratio mentioned above, we must ensure that the frame is stable. In case the story mechanism was observed, even if the relative story displacement limit was not reached, the analyses were terminated.

It is worth to mention that based on the results of experimental work performed on the frame-slit panel, the strength reduction was less than 80% for up to 7% drift [12] (Fig. 7). Also, no cracking and tearing up to 2.5% drift can be observed in the steel slit panel [6,19].

These control limits are provided on the pushover curves of the 6-story and 15-story structures (Fig. 14). For example, in the pushover curve of the 6-story structure, the first plastic hinge in the columns occurred when the roof displacement was 0.26 m. Additionally, when the roof displacement reached 0.41 m, the inter-story drift in the third story was 2%. Therefore, the first criterion, which happened earlier, was chosen to stop the analysis. In other structures, the criteria for stopping the analysis was also the formation of the plastic hinge in the columns, since it happened earlier.

7.3. Overstrength factors

To determine the overstrength factors, the roof displacement-base shear curves obtained from pushover analysis were used. For this purpose, the straight line was plotted in a way that the area under the actual and the idealized curve were equal as proposed in FEMA-356 [25] for the structures with positive post-yield stiffness (Fig. 16).

It is not allowed that the yield strength of the idealized force-displacement curve is more than the maximum base shear force of the actual curve [8]. The overstrength factors are plotted in Fig. 17a. It can be observed that the overstrength factors of the structures decrease up to 6 stories, and remain constant so after as the number of stories increases.

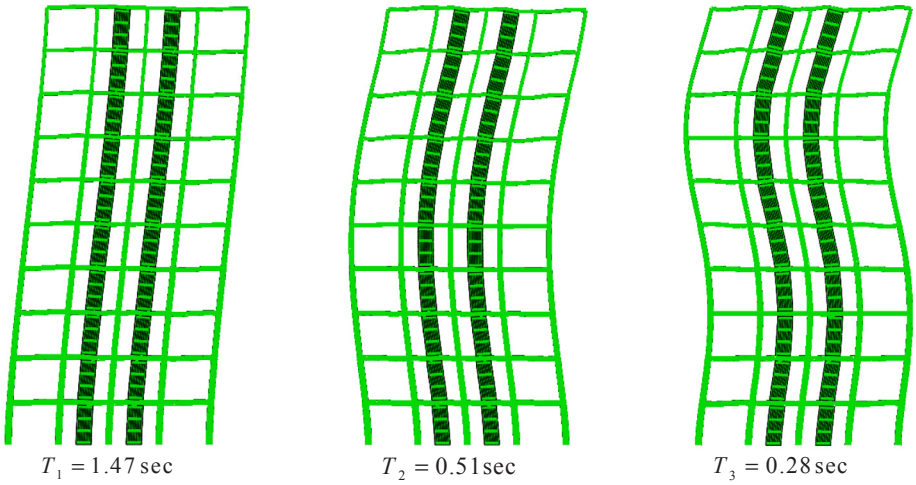

Fig. 19. Mode shapes and corresponding periods.

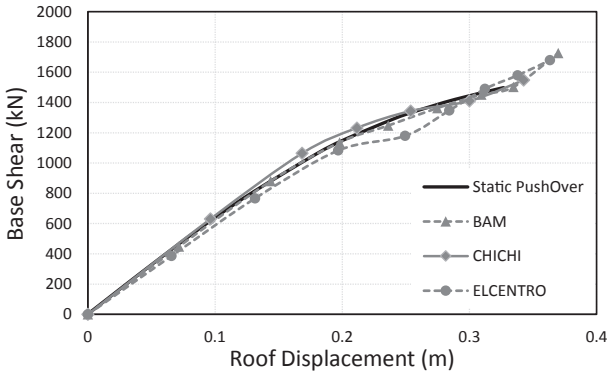

Fig. 20. Comparison of incremental dynamic and static pushover roof displacement-base shear curves of 10-story SSP-MRF.

Table 8
Results of incremental dynamic analyses of the 10-story SSP-MRF.

Earthquake	V_s (kN)	V_y (kN)	V_e (kN)	R_0	R_μ	R
Bam	237.65	1441.63	1925.64	6.07	1.33	8.07
Chichi	279.2	1445.32	1965.63	5.18	1.36	7.04
Elcentro	250.21	1337.72	1852.23	5.35	1.38	7.38

Table 9
Comparison of overstrength, ductility and response modification factors from incremental dynamic and pushover analysis.

parameters	Pushover analysis	Incremental dynamic analysis
R_0	3.75	5.53
R_μ	1.71	1.36
R	6.41	7.49

7.4. Ductility reduction factors

As mentioned, the ductility reduction factor is calculated according to Eq. (8). The global nonlinear response of a structure due to the energy dissipation is measured by this parameter [26]. The ductility factors are plotted in Fig. 17b. It is shown that the ductility factors of structures decrease as the number of stories increases up to 10 stories, and keep unchanged for higher structures.

7.5. Response modification factors

Once the overstrength and the ductility factors are obtained, the response modification factors are computed by multiplying two coefficients. The response modification factors are plotted in Fig. 18. It can be observed that the response modification factors of the structures decrease as the number of stories increases, and stayed almost constant in structures with more than 10-stories.

The overstrength, ductility and response modification factors for all moment-resistant frames with steel slit panel (SSP-MRFs) are shown in Table 6. In calculating these coefficients using pushover analyses, once the failure criteria (discussed in Section 7.2) were met by the analytical results, the analysis was terminated.

The overstrength and ductility factors were obtained as $R_0 = 4.16$ and $R_\mu = 1.91$, respectively. Final response modification factor for SSP-MRFs was calculated statically as R = 8.11 using the pushover analysis.

8. Comparison of pushover with incremental dynamic analysis results

Some incremental dynamic analyses using the time histories of Elcentro, Bam and Chichi (Table 7) which match with the design spectrum (Fig. 12) were carried out to evaluate the results of the nonlinear static analysis for the 10-story structure in Abaqus software. Mode shapes and periods of this structure are shown in Fig. 19. For the dynamic analysis, masses were calculated in a way that the period of SSP-MRF model was equal to the period of building. The masses were then placed over the beam in the story levels. The effective seismic mass was considered in accordance with Iranian Standard No. 2800 [10] (dead load and 20% of live load).

The PGAs of these records are changed using series of try and error in a way that the obtained time history results in the structure reaching to one of the pre-defined limit states.

The comparison of incremental dynamic analysis results and the static pushover curve in terms of roof displacement-base shear is presented in Fig. 20. The results of all earthquake excitations are well matched with static pushover curve, except for Elcentro record, which is different only at displacements ranging from 0.2 to 0.28 m. This may be due to Elcentro frequency content.

To obtain the response modification factors, three dynamic pushover envelopes were fitted into a bi-linear curve. The results of the incremental dynamic analysis are shown in Table 8. The overstrength, ductility reduction and response modification factors obtained by incremental dynamic analyses are 5.53, 1.36 and 7.49, respectively. Furthermore, these factors are compared with static pushover results

for the 10-story structure in Table 9.

9. Conclusions

The overstrength, ductility and response modification factors of dual moment-resistant frame system with steel slit panel with different stories were calculated using static pushover analyses. Some of the results were compared with the nonlinear incremental dynamic analyses. The results of the study can be summarized as follows:

1. The obtained overstrength factor of a moment resisting frame with steel slit panel is 4.16.
2. The obtained ductility factor of a moment resisting frame with steel slit panel is 1.91.
3. The response modification factor of a moment resisting frame with steel slit panel is 8.11.
4. The overstrength, ductility and response modification factors of a 10-story structure obtained by incremental dynamic analyses are 5.53, 1.36 and 7.49 respectively.
5. Overstrength factors decrease as the number of stories increases up to 6 stories and keep unchanged for structures with a higher number of stories.
6. Ductility factors decrease as the number of stories increases up to 10 stories, and remain unchanged for higher structures.
7. Response modification factors decrease as the number of stories increases and stay almost constant in more than 10-story structure.

Appendix A. Supplementary material

Supplementary data to this article can be found online at https://doi.org/10.1016/j.engstruct.2018.12.027.

References

[1] Anwar N. Behavior, modeling and design of shear wall-frame systems. Asian center for engineering computations and software; 2009.
[2] Mutoh K, Miyashita O, Osada M, Kanayama H. Stress and deformation of slit wall, using FEM. Summaries of technical papers of annual meeting Chugoku, Japan: AIJ; 1968. p. 543–4.
[3] Kwan A, Dai H, Cheung Y. Non-linear seismic response of reinforced concrete slit shear walls. J Sound Vib 1999;226:701–18.
[4] Muto K, Ohmori N, Takahashi T. A study on reinforced concrete slitted shear walls for high-rise buildings. Proceedings 5th world conference on earthquake engineering. 1973.
[5] Hitaka T, Matsui C, Sakai Ji. Cyclic tests on steel and concrete-filled tube frames with Slit Walls. Earthq Eng Struct Dyn 2007;36:707–27.
[6] Hitaka T, Matsui C. Experimental study on steel shear wall with slits. J Struct Eng, ASCE 2003;129(5):586–95.
[7] Cortés G, Liu J. Analytical investigation of steel slit panels for lateral resistance of steel frame proceedings for the ASCE structures congress 2008: crossing borders 2008. p. 1–5.
[8] Kim J, Choi H. Response modification factors of chevron-braced frames. Eng Struct 2005;27:285–300.
[9] Asgarian B, Shokrgozar H. BRBF response modification factor. J Constr Steel Res 2009;65:290–8.
[10] BHRC. Iranian code of practice for seismic resistant design of buildings: Standard no. 2800 (4rd editio). Building and Housing Research Center; 2015.
[11] MHUD. Iranian National Building Code, Part 10, steel structure design. Tehran (Iran): Ministry of Housing and Urban Development; 2013.
[12] Cortes G, Liu J. Experimental evaluation of steel slit panel–frames for seismic resistance. J Constr Steel Res 2011;67:181–91.
[13] McCloskey DM. Steel slit panels for lateral resistance of steel frame buildings MS. thesis West Lafayette (IN): Department of Civil Engineering, Purdue University; 2006.
[14] ATC. Structural response modification factors. ATC-19. Redwood City (CA): Applied Technology Council; 1995. p. 5–32.
[15] Uang CM. Establishing R (or R w) and C d factors for building seismic provisions. J Struct Eng 1991;117:19–28.
[16] He L, Togo T, Hayashi K, Kurata M, Nakashima M. Cyclic behavior of multirow slit shear walls made from low-yield-point steel. J Struct Eng 2016;142:04016094.
[17] Khatamirad M, Shariatmadar H. Experimental and analytical study of steel slit shear wall. Steel Compos Struct 2017;24.
[18] Garivani S, Aghakouchak A, Shahbeyk S. Numerical and experimental study of comb-teeth metallic yielding dampers. Int J Steel Struct 2016;16:177–96.
[19] Cortes G. Steel slit panel frames for lateral resistance of buildings Ph. D. dissertation West Lafayette (IN): Department of Civil Engineering, Purdue University; 2009.
[20] Wang M, Yang W, Shi Y, Xu J. Seismic behaviors of steel plate shear wall structures with construction details and materials. J Constr Steel Res 2015;107:194–210.
[21] Shi Y, Wang M, Wang Y. Experimental and constitutive model study of structural steel under cyclic loading. J Constr Steel Res 2011;67:1185–97.
[22] ATC. guidelines for cyclic seismic testing of components of steel structures. ATC-24. Redwood City (CA): Applied Technology Council;1992.
[23] ABAQUS V. 6.14 Documentation. Dassault Systemes Simulia Corporation; 2014.
[24] Mwafy A, Elnashai A. Static pushover versus dynamic collapse analysis of RC buildings. Eng Struct 2001;23:407–24.
[25] FEMA. Commentary for the seismic rehabilitation of buildings. FEMA-356. Washington, D.C.: Federal Emergency Management Agency; 2000.
[26] Mahmoudi M, Abdi MG. Evaluating response modification factors of TADAS frames. J Constr Steel Res 2012;71:162–70.